

A Study of Three Dimensional Numerical Analysis on Vacuum Consolidation

Chung, Youn-In*

요 지

본 연구에서는 유한변형률 이론에 근거하여 3차원 압밀 지배 방정식을 유도하였다. 이 방정식은 비교적 압밀층의 두께가 두꺼운 경우, 비선형 물성치, 공극비에 따른 비선형 투수계수를 갖는 지반에 적합하다. 기존의 유한 차분 수치해석 기법(FTCS)은 지배 방정식이 비선형이며 복잡한 경우 안정된 해를 얻을 수 없기 때문에 본 연구에서는 특수 유한 차분 기법을 도입하였다. 이 수치해석 기법을 지배 방정식에 적용하면 시간에 따른 압밀량을 예측할 수 있다. 본 해석 기법에 의해 구해진 값들을 워드레인을 설치한 여러 가지 고압축성 토질에서의 실험 결과와 비교한 결과, 최종 압밀량과 시간에 따른 압밀량이 잘 일치하고 있다.

Abstract

A governing equation of uncoupled three dimensional finite strain theory of consolidation is presented. This equation is suitable for relatively thick layers, possessing large strain, non-linear material property, and variable permeability. A special numerical solution procedure has to be adopted for the finite difference scheme because the solution is not stable in using Forward-Time Centered-Space (FTCS) method and the governing equation is highly non-linear. The solution is capable of predicting settlement with respect to time. The results predicted by the developed method of analysis have been compared with those of experimental tests on different types of highly compressible soils with vertical wick drain. The uncoupled three dimensional finite strain theory of consolidation appears to predict settlement behavior well. A detailed comparison shows good agreement in terms of total settlement, and reasonable agreement with respect to time.

Keywords : Vacuum consolidation, Finite strain theory, Void ratio, Wick drain, Compressible soil

1. Introduction

Terzaghi's theory of one dimensional consolidation is widely used to analyze the consoli-

* Member, Assistant Professor, Dept. of Civil Eng., Keimyung University, Daegu, Korea

dating of saturated clay. Although this theory is considered to be an accepted method of analyzing consolidation, it is recognized as an oversimplification of the true field behavior. Terzaghi's theory is restricted in its applicability to a relatively thin layer with infinitesimal strains and a linear stress-strain material property relationship. Infinitesimal strain consolidation theory is based on the assumption that the deformation of the consolidating layer is small compared to its thickness. Therefore, the deformation of the consolidating layer can be neglected during the process of consolidation, that is, the thickness of the layer is assumed constant throughout the consolidation process. In the infinitesimal strain consolidation theory, it is also assumed that both the permeability and compressibility of the soil remain constant during consolidation under a particular increment of the load. However, for highly compressible soils, deformations are large compared with the thickness of the layer. Clearly, errors arise from such assumptions. As a result, a number of researchers have focused on the non-linear behavior of soil to extend the classical theory during consolidation. In this paper, a mathematical model is developed to characterize the finite strain consolidation which reconsiders some simplifying assumptions incorporated in the infinitesimal strain consolidation theory. The results predicted by the developed method of analysis are compared with those from the experimental tests on five different types of soils. The comparisons show in general good agreement in terms of settlement with respect to time.

2. Coordinate Systems and Transformations

In the finite strain theory of consolidation, the strain is so large that the thickness of the compressible layer decreases while time increases. Therefore the coordinate system is an important aspect in the finite strain theory of consolidation.

2.1 Lagrangian Coordinate System

The Lagrangian system is the initial configuration of the clay layer before consolidation begins; it is time-independent, and refers all events to an initial $t=0$ configuration. A clay layer has an initial configuration as shown in Fig. 1-a. A sample of the clay layer (AoBoCoDo) has a coordinate position ζ and has thickness $\delta\zeta$. The bottom boundary is at $\zeta=0$ and the upper boundary is at $\zeta=\zeta_0$. The distance ζ is the Lagrangian coordinate. With consolidation the clay layer will have a new configuration shown in Fig. 1-b. The top surface has moved and the sample has deformed to a new position (ABCD) while the bottom surface is fixed. A new distance ξ locates a material point as a function of time; the distance ξ is the convective coordinate which is a function of the position in space and time. It is therefore convenient to express the dependent variable to be calculated in terms of the convective coordinate ξ and time. However, this is mathematically complicated because ξ itself is a function of coordinate ζ and time t . The initial coordinate system ζ is, how-

ever, independent of time and ζ along with t is an independent variable. Therefore the mathematics of finite strain consolidation is simplified by working in the (ζ, t) system which is a Lagrangian coordinate system.

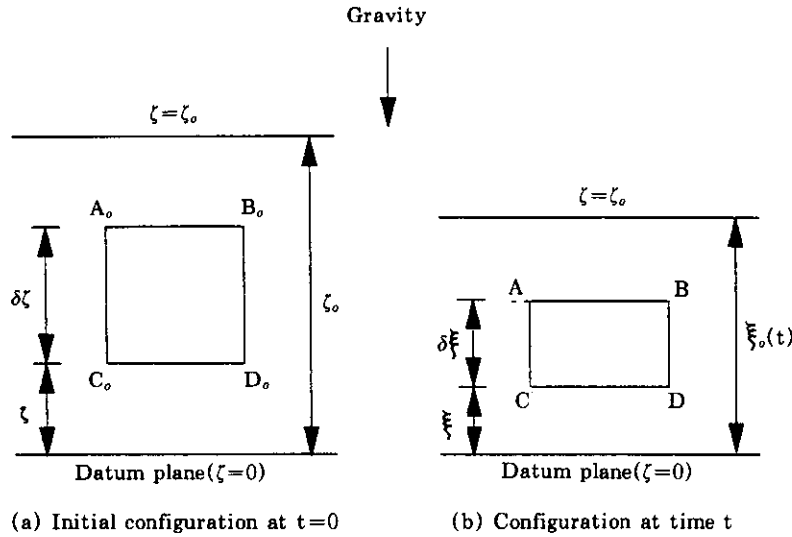


Fig.1 Lagrangian and convective coordinate (after Gibson, 5)

2.2 Material (Reduced) Coordinate System

The Material (Reduced) coordinate is based on the volume of the soil particles lying between the datum plane and the point being analyzed. This coordinate z is defined as

$$z(\zeta) = \int_0^\zeta [1 - n(\zeta, 0)] d\zeta \quad (1)$$

where n = porosity of soil

As with the ζ coordinate the point z is independent of time. The porosity, n , may be expressed in terms of void ratio, e , then Eqn. (1) becomes

$$z(\zeta) = \int_0^\zeta \frac{d\zeta}{1 + e(\zeta, 0)} \quad (2)$$

2.3 Coordinate Transformations

Consider a soil element with consolidation as shown in Fig. 2. In the initial state ($t=0$), the element is composed of a unit volume of solids and volume of void which is equal to the initial void ratio e_0 with an initial thickness $\delta\zeta$. With consolidation ($t>0$), the element has consolidated to a smaller thickness $\delta\xi$ with the same unit volume of solids ($\gamma_s = \text{constant}$) while decreasing volume of voids designated by the void ratio e as explained in Fig. 2-a. Since there is no lateral strain, the ratio of $\delta\zeta$ to $\delta\xi$ becomes

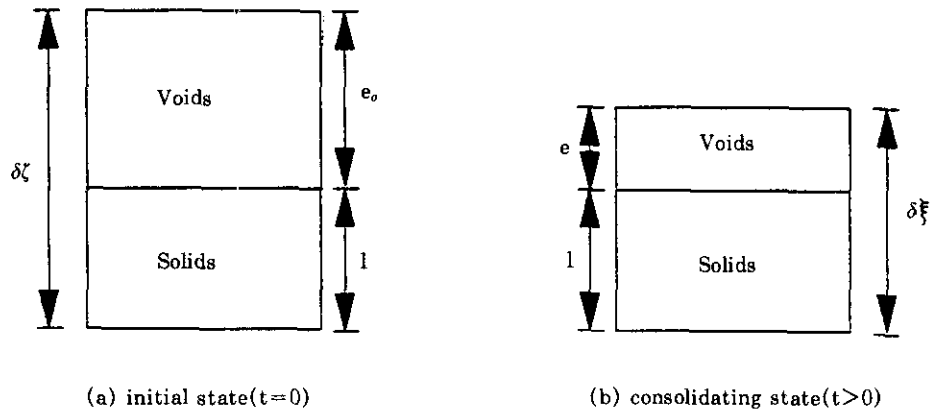


Fig.2 Changes in void ratio during consolidation(after Gibson, 5)

$$\frac{\partial \zeta}{\partial \xi} = \frac{1+e_0}{1+e} \quad (3)$$

where e is a function of ζ and t

ξ = convective coordinate system

The transformation relationship between ζ and z coordinate can be derived by differentiating Eqn. (2)

$$\frac{dz}{d\zeta} = \frac{1}{1+e(\zeta, 0)} \quad (4)$$

The transformation relationship between z and ξ coordinates is given by

$$\frac{dz}{d\xi} = \frac{1}{1+e} \quad (5)$$

Eqn. (3), Eqn. (4), and Eqn. (5) are the necessary transformed relationship between the coordinates. Gibson, England, and Hussey and Gibson, Schiffman, and Cargill contribute to the development and application of these coordinate systems.

3. Uncoupled Three Dimensional Finite Strain Theory

Zhao described the governing equation for uncoupled three dimensional finite consolidation. This theory is based on one dimensional finite strain consolidation theory of Gibson et. al. The material coordinate was used to simplify the analytical formulation involved.

A general three dimensional finite strain consolidation equation becomes

$$\begin{aligned} & \pm \left(\frac{\gamma_s}{\gamma_w} - 1 \right) \frac{d}{de} \left(\frac{k_z(e)}{1+e} \right) \frac{\partial e}{\partial z} + \frac{\partial}{\partial z} \left(\frac{k_z(e)}{\gamma_w(1+e)} \frac{d\sigma'_z}{de} \frac{\partial e}{\partial z} \right) \\ & + (1+e_0) \frac{d}{dx} \left(-\frac{k_x(e)}{\gamma_w} \frac{du}{dx} \right) + (1+e_0) \frac{d}{dy} \left(-\frac{k_y(e)}{\gamma_w} \frac{du}{dy} \right) + \frac{\partial e}{\partial t} = 0 \end{aligned} \quad (6)$$

where u = pore fluid pressure and $k_x(e)$, $k_y(e)$, and $k_z(e)$ are the permeability coefficients in x , y , and z directions, respectively. It was assumed that soil has isotropic permeability,

$$k_x(e) = k_y(e) = k_z(e) = k(e) \quad (7)$$

This governing equation appears to be highly nonlinear. To simplify Eqn. (6), the parameters introduced by Gibson et. al. were adopted,

$$g(e) = -\frac{k(e)}{\gamma_w} \frac{1}{(1+e)} \frac{d\sigma'_z}{de} \quad (8)$$

$$\lambda(e) = -\frac{d}{de} \left(\frac{de}{d\sigma'_z} \right) \quad (9)$$

The $g(e)$ and $\lambda(e)$ were assumed to be constants and the relationship between void ratio and effective stress is

$$e = (e_{00} - e_z) \exp(-\lambda \sigma'_z) + e_z \quad (10)$$

or

$$\sigma'_z = \frac{1}{\lambda} \ln \left(\frac{e - e_z}{e_{00} - e_z} \right) \quad (11)$$

Differentiation of Eqn. (11) yields

$$d\sigma'_z = -\frac{1}{\lambda} \frac{1}{e - e_z} de \quad (12)$$

The decrease in pore fluid pressure is equal to the increase in effective stress,

$$du = -d\sigma'_z \quad (13)$$

Substitution of Eqn. (13) into Eqn. (12) yields

$$du = \frac{1}{\lambda} \frac{1}{e - e_z} de \quad (14)$$

Multiplying Eqn. (14) by $\frac{k_x(e)}{\gamma_w} \frac{1}{dx}$ and assuming that soil has isotropic permeability, the following expression is obtained,

$$\frac{k_x(e)}{\gamma_w} \frac{du}{dx} = \frac{k(e)}{\gamma_w \lambda (e - e_z)} \frac{de}{dx} \quad (15)$$

Similarly,

$$\frac{k_y(e)}{\gamma_w} \frac{du}{dy} = \frac{k(e)}{\gamma_w \lambda (e - e_z)} \frac{de}{dy} \quad (16)$$

Substitution of Eqn. (8), (9), (15), and Eqn. (16) into Eqn. (6) yields

$$\begin{aligned} & \mp (\gamma_s - \gamma_w) g \lambda \frac{\partial e}{\partial z} + g \frac{\partial^2 e}{\partial z^2} \\ & + \frac{(1+e_0)}{\gamma_w \lambda} \frac{d}{dx} \left(\frac{k(e)}{(e - e_z)} \frac{de}{dx} \right) + \frac{(1+e_0)}{\gamma_w \lambda} \frac{d}{dy} \left(\frac{k(e)}{(e - e_z)} \frac{de}{dy} \right) = \frac{de}{dt} \end{aligned} \quad (17)$$

By considering $\frac{d}{dx} \left(\frac{k(e)}{(e - e_z)} \frac{de}{dx} \right)$ in Eqn. (17), one can have,

$$\frac{d}{dx} \left(\frac{k(e)}{(e-e_x)} \frac{de}{dx} \right) = \frac{d}{dx} \left(\frac{k(e)}{e-e_x} \right) \frac{de}{dx} + \frac{k(e)}{(e-e_x)} \frac{d^2e}{dx^2} \quad (18)$$

By taking $\frac{d}{dx} \left(\frac{k(e)}{e-e_x} \right)$ in Eqn. (18), one can have,

$$\frac{d}{dx} \left(\frac{k(e)}{e-e_x} \right) = \frac{1}{(e-e_x)} \frac{dk(e)}{dx} - \frac{k(e)}{(e-e_x)^2} \frac{de}{dx} \quad (19)$$

Then, by the mathematical process,

$$\frac{d}{dx} \left(\frac{k(e)}{(e-e_x)} \frac{de}{dx} \right) = \frac{1}{(e-e_x)} \frac{dk(e)}{dx} \frac{de}{dx} - \frac{k(e)}{(e-e_x)^2} \left(\frac{de}{dx} \right)^2 + \frac{k(e)}{(e-e_x)} \frac{d^2e}{dx^2} \quad (20)$$

Similarly,

$$\frac{d}{dy} \left(\frac{k(e)}{(e-e_x)} \frac{de}{dy} \right) = \frac{1}{(e-e_x)} \frac{dk(e)}{dy} \frac{de}{dy} - \frac{k(e)}{(e-e_x)^2} \left(\frac{de}{dy} \right)^2 + \frac{k(e)}{(e-e_x)} \frac{d^2e}{dy^2} \quad (21)$$

Substitution of Eqn. (20) and (21) into Eqn. (17) yields

$$\begin{aligned} \frac{de}{dt} = & \mp (\gamma_s - \gamma_w) g \lambda \frac{\partial e}{\partial z} + g \frac{\partial^2 e}{\partial z^2} \\ & + \frac{(1+e_0)}{\gamma_w \lambda} \left(\frac{1}{e-e_x} \frac{dk}{dx} \frac{de}{dx} - \frac{k}{(e-e_x)^2} \left(\frac{de}{dx} \right)^2 + \frac{k}{e-e_x} \frac{d^2e}{dx^2} \right) \\ & + \frac{(1+e_0)}{\gamma_w \lambda} \left(\frac{1}{e-e_x} \frac{dk}{dy} \frac{de}{dy} - \frac{k}{(e-e_x)^2} \left(\frac{de}{dy} \right)^2 + \frac{k}{e-e_x} \frac{d^2e}{dy^2} \right) \end{aligned} \quad (22)$$

It should be noted that Eqn. (22) is completely uncoupled three dimensional governing equation of the finite strain theory of consolidation along x, y, and z coordinate. Also, Eqn. (22) is suitable for relatively thick layers, possessing large strains, and variable permeability.

4. Numerical Analysis

The uncoupled three dimensional finite strain formulation developed in previous section is applied to the solution of vacuum consolidation of highly compressible soil with vertical wick drain. In order to solve the governing equation developed in section 3 and to establish a more efficient solution, an explicit finite difference scheme is adopted. However, the ordinary explicit finite difference scheme (Forward-Time Centered-Space method) is not suitable for this case because the governing equation is highly non-linear and the solution is not stable. A special finite difference scheme, Dufort-Frankel finite difference method, is used to eliminate the problem of instability because this method is unconditionally stable.

4.1 Consolidation by Wick Drain

Typical arrangements of the round-shaped wick drains are shown in Fig. 3. However, the area of wick drain is very small compared to the zone of influence. Therefore, the portion of wick drain is assumed a dot (no area) in numerical analysis. Actual vacuum experiment test had cylindrical soil height, however, in the numerical analysis, the zone of influence of

wick drain is assumed as square shape shown in Fig. 3. Therefore, the area of round shaped influence zone should be converted to the area of square shaped influence zone by Eqn. (23).

$$s^2 = \frac{\pi}{4} d_w^2 \quad (23-a)$$

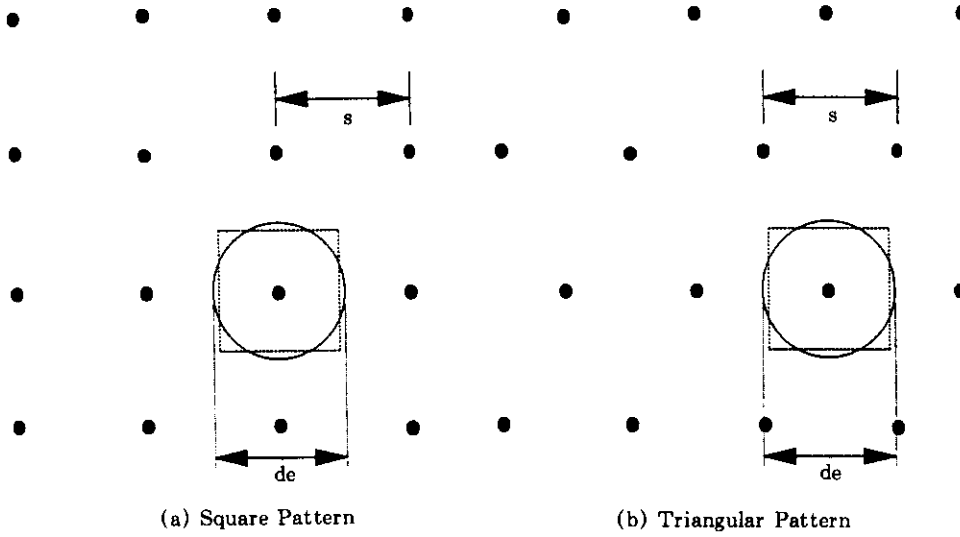


Fig.3 Horizontal arrangement of round shaped wick drain

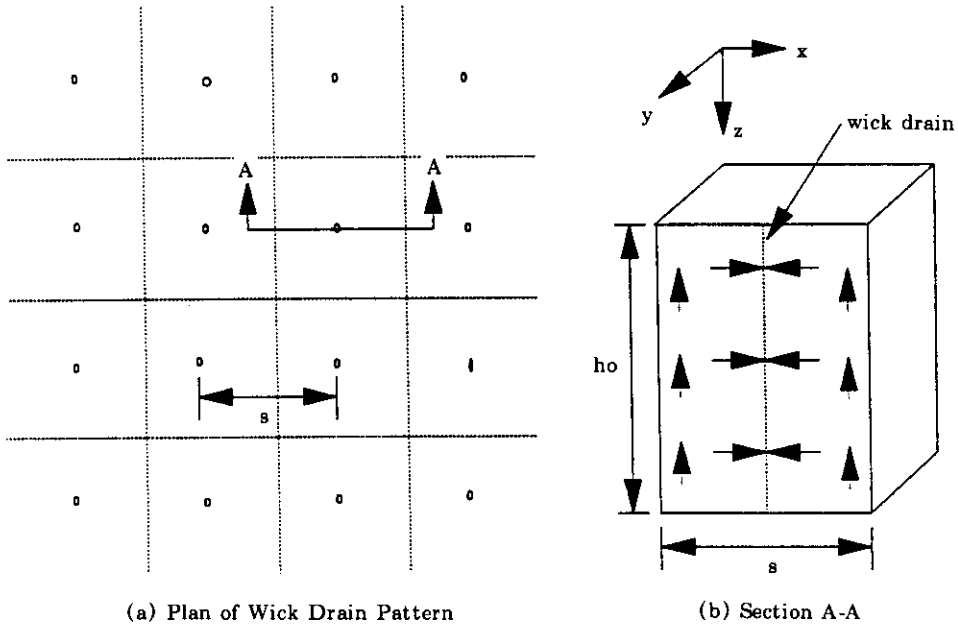


Fig.4 Fundamental concept of wick drain

or

$$s = 0.89d_e \tag{23-b}$$

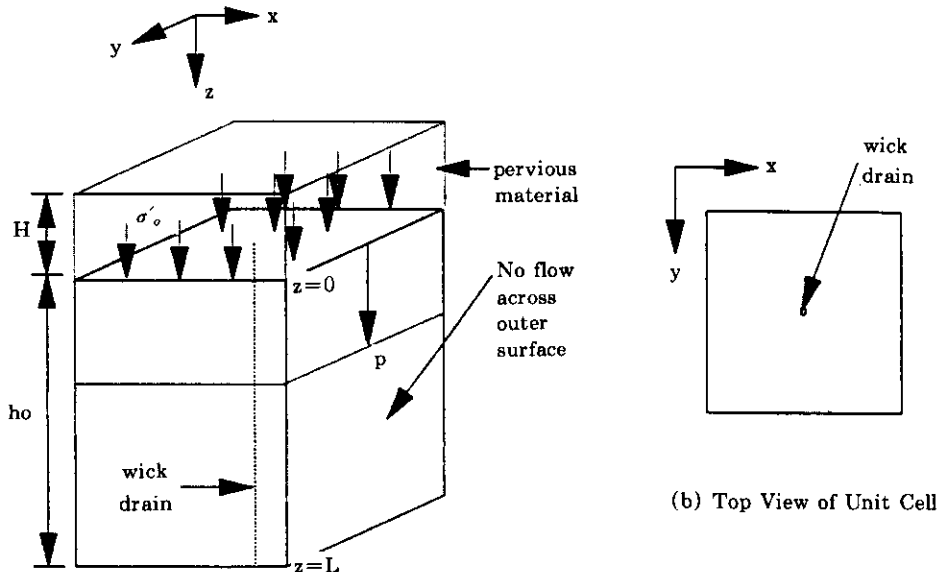
where s = spacing of square shaped wick drain

d_e = diameter of the zone of influence

The problem domain consists of the entire grid pattern shown in Fig. 4. Using the unit cell concept, the solution domain is reduced from the problem domain to a single representative square (unit cell).

4.2 Boundary Conditions

Referring to Fig. 5, the clay layer with an initial thickness, h_0 , is fully consolidated and is in equilibrium under both its own weight and a vertical effective stress σ'_0 acting on its upper surface. The soil is fully saturated and water table is assumed at a distance H above its upper surface. The upper surface of the clay layer is in contact with a pervious soil. The wick drain is assumed to be driven to the bottom of the clay layer. Since the permeability was assumed isotropic in all directions and it is assumed each wick drain is equally effective, flow to any wick drain will be bounded by the four sides of square unit cell. Therefore, the four sides of unit cell may be assumed impervious in the analyses. The middle of the unit cell is the wick drain boundary. This boundary is the soil-drain interface, and is assumed freely drained. The lower surface of the clay is in contact with impervious layer. In this analysis, the reduced coordinate, z , is defined positive downward from the upper surface. The upper surface serves as a moving datum and so the positive sign must be taken in Eqn. (22). The governing equation will then become



(a) The Height of Unit Cell

Fig.5 View of unit cell

$$\begin{aligned}
\frac{de}{dt} &= (\gamma_s - \gamma_w) g \lambda \frac{\partial e}{\partial z} + g \frac{\partial^2 e}{\partial z^2} \\
&+ \frac{(1+e_0)}{\gamma_w \lambda} \left(\frac{1}{e-e_x} \frac{dk}{dx} \frac{de}{dx} - \frac{k}{(e-e_x)^2} \left(\frac{de}{dx} \right)^2 + \frac{k}{e-e_x} \frac{d^2 e}{dx^2} \right) \\
&+ \frac{(1+e_0)}{\gamma_w \lambda} \left(\frac{1}{e-e_x} \frac{dk}{dy} \frac{de}{dy} - \frac{k}{(e-e_x)^2} \left(\frac{de}{dy} \right)^2 + \frac{k}{e-e_x} \frac{d^2 e}{dy^2} \right)
\end{aligned} \tag{24}$$

Eqn. (24) is the final form of the governing equation used to develop the computer program. Note that Eqn. (24) is completely uncoupled along the x and y (horizontal) coordinate, and z (vertical) coordinate.

4.2.1 Initial Void Ratio Through the Soil Layer

Since z is the volume of solids between the datum plane and a plane through the point p shown in Fig. 5.a, the initial vertical effective stress becomes

$$\sigma'(x, y, z)_{t=0} = \sigma'_0 + (\gamma_s - \gamma_w)z \tag{25}$$

By substituting Eqn. (25) into Eqn. (10) with $\sigma'_0 = 0$ (that is, initial effective stress at the top surface equals zero), the void ratio varies initially through the layer according to the equation

$$e(x, y, z)_{t=0} = (e_{00} - e_x) \exp\{-\lambda(\gamma_s - \gamma_w)z\} + e_x \tag{26}$$

4.2.2 Void Ratios at Upper Surface

If an external vertical load Δq is applied suddenly on the soil surface, the effective stress immediately increases by Δq at upper surface ($z=0$). In this circumstance, the boundary condition of the upper surface becomes

$$e(x, y, 0)_{t=t_1} = (e_{00} - e_x) \exp\{-\lambda[\sigma'_0 + \Delta q]\} + e_x \tag{27}$$

4.2.3 Void Ratios at Wick Drain

Since the wick drain-soil interface is assumed freely drained, the total stress at the boundary of wick drain equals the effective stress at any time. Therefore, the boundary condition of the wick drain becomes

$$e(x/2, y/2, z)_{t=t_1} = \{e(x, y, 0)_{t=t_1} - e_x\} \exp\{-\lambda(\gamma_s - \gamma_w)z\} + e_x \tag{28}$$

4.2.4 Void Ratios at Boundaries of Four Sides of Unit Cell

As mentioned previously, the four sides of unit cell may be assumed as impervious boundary. Referring to Fig. 5.a, the boundary conditions of four sides of unit cell require

1) side 1 ($x=x, y=0, z=z$)

$$\frac{\partial e}{\partial y} = 0 \tag{29}$$

2) side 2 ($x=x, y=s, z=z$)

$$\frac{\partial e}{\partial y} = 0 \tag{30}$$

3) side 3 ($x=0, y=y, z=z$)

$$\frac{\partial e}{\partial x} = 0 \quad (31)$$

4) side 4 ($x=s, y=y, z=z$)

$$\frac{\partial e}{\partial x} = 0 \quad (32)$$

4.2.5 Void Ratios at Bottom Surface

At the lower boundary ($z=L$), an impervious condition requires

$$V_{wz} = V_s \quad (33)$$

where V_{wz} = vertical velocity of the pore water

V_s = vertical velocity of the solid phase

The equation of equilibrium of the water and solid mixture in the soil may be expressed as:

$$\frac{\partial \sigma_z}{\partial z} = -(\gamma_s + e\gamma_w) \quad (34)$$

Also the equation of modified Darcy's law may be expressed as:⁽¹³⁾

$$n(V_{wz} - V_s) + k_z + \frac{k_z}{\gamma_w(1+e)} \frac{\partial u}{\partial z} = 0 \quad (35)$$

where n = porosity of soil

u = pore water pressure

Substitution of Eqn. (33) into Eqn. (35) yields

$$\frac{\partial u}{\partial z} = -\gamma_w(1+e) \quad (36)$$

The effective stress equation is

$$u = \sigma_z - \sigma'_z \quad (37)$$

where σ_z = total vertical stress of soil

σ'_z = effective vertical stress of soil

Differentiation of Eqn. (37) with respect to z yields

$$\frac{du}{dz} = \frac{d\sigma_z}{dz} - \frac{d\sigma'_z}{dz} \quad (38)$$

From Eqn. (36), Eqn. (38) becomes

$$\frac{d\sigma_z}{dz} - \frac{d\sigma'_z}{dz} = -\gamma_w(1+e) \quad (39)$$

The combination of Eqn. (34) and Eqn. (39) yields

$$\frac{d\sigma'_z}{dz} + (\gamma_s - \gamma_w) = 0 \quad (40)$$

By the chain rule

$$\frac{d\sigma'_z}{dz} = \frac{d\sigma'_z}{de} \frac{de}{dz} \quad (41)$$

Substitution of Eqn. (41) into Eqn. (40) yields

$$\frac{\partial e}{\partial z} + (\gamma_s - \gamma_w) \frac{de}{d\sigma'_z} = 0 \quad (42)$$

From Eqn. (12),

$$d\sigma'_z = -\frac{1}{\lambda(e - e_x)} de \quad (12)$$

one can obtain

$$\frac{de}{d\sigma'_z} = -\lambda(e - e_x) \quad (43)$$

Substitution of Eqn. (43) into Eqn. (42) yields

$$\frac{\partial e}{\partial z} - \lambda(\gamma_s - \gamma_w)(e - e_x) = 0 \quad (44)$$

Eqn. (44) becomes the boundary condition of bottom surface.

4.3 Settlement - Time Relationship

The change in thickness δS of an element of the soil skeleton at time t is

$$\delta S = \left[1 - \frac{\partial \xi}{\partial \zeta}\right] \delta \zeta \quad (45)$$

so that the settlement S of the entire stratum along any soil column ($x=x_i, y=y_j, z=z_k$) is

$$S(x, y, z)_{t=t} = \int_0^{h_0} \left[1 - \frac{\partial \xi}{\partial \zeta}\right] \delta \zeta \quad (46)$$

Using Eqn. (3), (4), and Eqn. (46), settlement can be expressed as

$$S(x, y, z)_{t=t} = \int_0^L [e(x, y, z)_{t=0} - e(x, y, z)_{t=t}] dz \quad (47)$$

$$= [e(x, y, z)_{t=0} - e(x, y, z)_{t=t}] L \quad (48)$$

By the definition of material coordinate

$$L = \frac{h_0}{1 + e_0} \quad (49)$$

where e_0 = average initial void ratio

h_0 = initial height

L = height of soil in material coordinate

Substitution of Eqn. (49) into Eqn. (48) yields

$$S(x, y, z)_{t=t} = [e(x, y, z)_{t=0} - e(x, y, z)_{t=t}] \frac{h_0}{1 + e_0} \quad (50)$$

The average settlement for all the soil columns, i. e. , the settlement of the entire soil layer is

$$S_{ave}(t) = \frac{1}{(N_x N_y N_z)} \sum_{i=1}^{N_x} \sum_{j=1}^{N_y} \sum_{k=1}^{N_z} [e(x_i, y_j, z_k)_{t=0} - e(x_i, y_j, z_k)_{t=t}] \frac{h_0}{1 + e_0} \quad (51)$$

where N_x = the number of points along x direction

N_y = the number of points along y direction

N_k = the number of points along z direction

S_{ave} = average calculated settlement of all node at time = t

At the end of consolidation ($t \rightarrow \infty$), the maximum settlement is achieved as follows

$$S_{ave}(\infty) = \frac{1}{(N_i N_j N_k)} \sum_{i=1}^{N_i} \sum_{j=1}^{N_j} \sum_{k=1}^{N_k} [e(x_i, y_j, z_k)_{t=0} - e(x_i, y_j, z_k)_{t \rightarrow \infty}] \frac{h_0}{1 + e_0} \quad (52)$$

where $S_{ave}(\infty)$ = average calculated settlement of all node at time $\rightarrow \infty$

Furthermore, the degree of consolidation at time t is expressed as the percentage of settlement

$$U(t) = \frac{S_{ave}(t)}{S_{ave}(\infty)} \quad (53)$$

4.4 Finite Difference Analysis

Finite difference scheme applied to the governing equation, boundary conditions, and the settlement-time relationship developed previously. Explicit DuFort-Frankel finite difference method is used to solve non-linear partial differential equations, system of partial differential equations, and multidimensional problems. This method is a three-level method which uses known values at $T - \Delta T$ and T to calculate unknown value at $T + \Delta T$, where 1) $T - \Delta T$ = one time level before current level, 2) T = current level, and 3) $T + \Delta T$ = one time level after current level. Therefore, two known values, $T - \Delta T$ and T , are required to start the method. However, initially the only known value is initial boundary condition value, T . The next step, $T + \Delta T$, is unknown. In order to calculate the value at $T + \Delta T$ a known value at $T - \Delta T$ is required. Since T is on the initial boundary of the system, $T - \Delta T$ is outside of the system. Consequently, the value at $T - \Delta T$ (imaginary time level) was set equal to the value at T . This, then, provides known values at $T - \Delta T$ and T . With the values of these two time levels, the values of third time level can be obtained by the explicit DuFort-Frankel method.

A computer program was written to perform the necessary calculation. This computer program can handle 14 columns along the x and y (horizontal) direction, and 30 layers along the z (vertical) direction. The nodes are $15 \times 15 \times 31$ within the boundaries. However, the boundaries of the four sides of a unit cell require a fictitious column beyond each side of the unit cell. Therefore, the maximum finite difference grid is $17 \times 17 \times 31$ in the computer program.

5. Results

In Fig. 6 through Fig. 10, Settlement-Time curves were drawn to compare the results of experiments on five different types of highly compressible soils with vertical wick drain⁽²⁾ with those of numerical analysis.

Soils were classified after laboratory testing in accordance with ASTM D-2487 "Classifi-

cation of Soils for Engineering Purpose". These classification are based on laboratory results on the actual samples tested and visual classification. The five different types of soil were classified as follow :

Table 1. Classification of soil sample

Soil	Classification	Description of soil
Soil #1	MH	Inorganic silts
Soil #2	MH	As above
Soil #3	MH	As above
Soil #4	CL	Lean clay with sand
Soil #5	CL	As above

The properties of soils and vacuum consolidation testings are not included in this paper. Those can be found in references ^{(2),(3)}

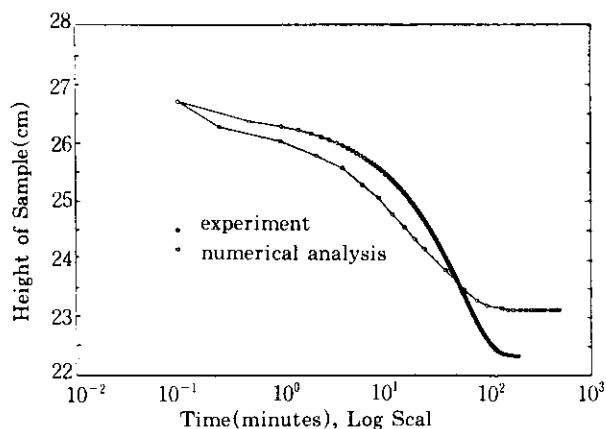


Fig.6 Comparison—experimental and numerical analysis for soil #1

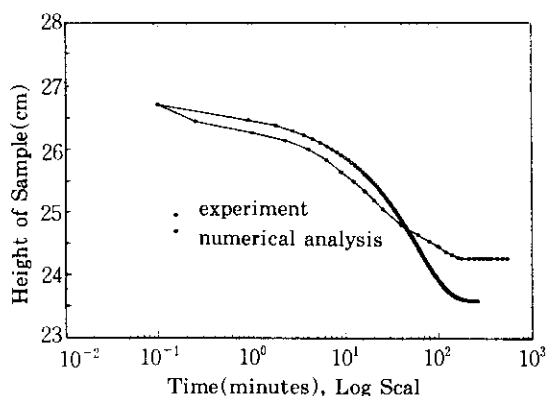


Fig.7 Comparison—experimental and numerical analysis for soil #2

1) soil #1

The numerical analysis predicts 7.5% slower than experiment in terms of time to reach ultimate settlement. The numerical analysis also estimates approximately 20% higher ultimate settlement than that measured experimentally.

2) soil #2

As can be seen from Fig. 7, the time to reach ultimate settlement is closely predicted by the numerical model. However, the numerical analysis estimates approximately 25% more settlement than was measured experimentally.

3) soil #3

As observed in Fig. 8, the numerical analysis for this soil predicts approximately 45% less time to reach ultimate settlement as compared to the experimental results. A possible

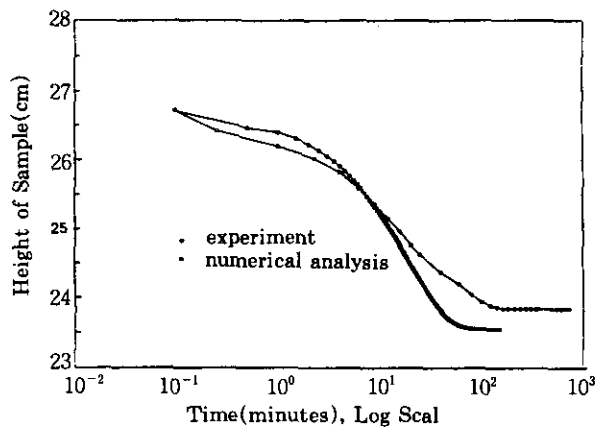


Fig.8 Comparison—experimental and numerical analysis for soil #3

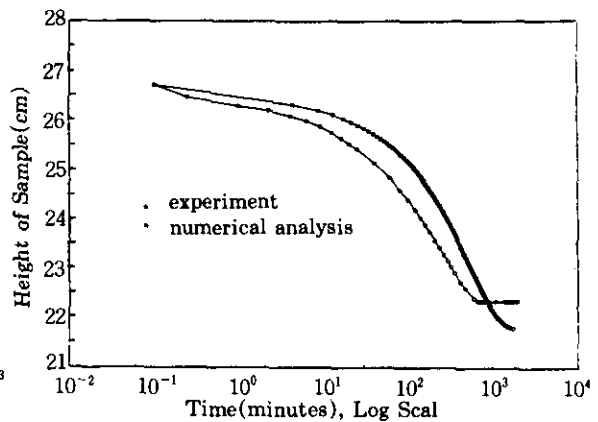


Fig.9 Comparison—experimental and numerical analysis for soil #4

reason for this is that the g values of this soil varied more than those for the other soil types in the experiment. Total settlements obtained analytically and experimentally agree well.

4) soil #4

As can be seen in Fig. 9, numerical analysis and the experimental results agree well. However, the analytical results predict a slightly higher time to reach ultimate settlement and a slightly higher total settlement.

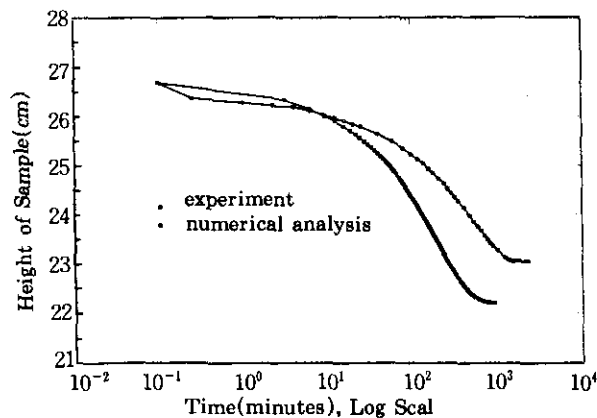


Fig.10 Comparison—experimental and numerical analysis for soil #5

5) soil #5

As can be seen in Fig. 10, the numerical analysis predicts approximately 35% less time to reach ultimate settlement and 20% more ultimate settlement compared to the experimentally measured values.

6. Conclusions

Based on the results of uncoupled three dimensional numerical analysis with finite strain theory of consolidation, it can be concluded that

- (1) The measured and calculated settlement are well compared with respect to time and ultimate settlement.
- (2) For all five different types of soil, numerical analysis estimates approximately 10 to 25% higher ultimate settlement than the experiment. The average ultimate settlement obtained from the numerical analysis was 18.9% higher than that obtained from the experiment.
- (3) The average difference in time to reach the ultimate settlement between experiment and numerical analysis is 50.8% because the g values, assumed as constant in numerical analysis, of soil #3 varied more than those for the other soil types in the experiment. Except for soil #3, the average difference in time to reach the ultimate settlement between experiment and numerical analysis is 27.6%.
- (4) The large difference between experiment and numerical analysis for soil #3 is mainly due to the values of g . When the values of g are reasonably adjusted, agreement between experiment and analytical results is excellent.

Acknowledgements

The present research has been conducted by the Bisa Research Grant of Keimyung University in 1995.

References

1. Berg, Jeanne A.(1992), "Vacuum Consolidation of Sludge", M. S. Thesis, South Dakota School of Mines and Technology, Rapid City, South Dakota, U.S.A.
2. Chung, Youn-In(1993), "Vacuum Consolidation of Highly Compressible Soil with Vertical Wick Drains", Ph. D Dissertation, South Dakota School of Mines and Technology, Rapid City, South Dakota, U.S.A.
3. Chung, Youn-In(1995), "Vacuum Consolidation on Highly Compressible Soil", Journal of the Korean Geotechnical Society, Vol. 11, No. 4.
4. Gibson, R. E., England, G. L., Hussey, M. J. L.(1967), "The Theory of One-Dimensional Consolidation of Saturated Clay, I. Finite Non-Linear Consolidation of Thin Homogeneous Layers", Geotechnique, 17.
5. Gibson, Robert E., Schiffman, Robert L. and Cargill, Kenneth W.(1981), "The Theory of One-Dimensional Consolidation of Saturated Clay, II. Finite Non-Linear Consolidation of Thick Homogeneous Layers", Canadian Geotechnical Journal, 18.
6. Hansbo, S.(1981), "Consolidation of Fine-Grained Soils by Prefabricated Drains", Proceeding of Tenth International Conference on Soil Mechanics and Foundation Engineering, Stockholm, Vol. 3.

7. Hoffman, Joe D.(1992), "Numerical Methods for Engineers and Scientists", McGraw Hill, Inc.
8. McNabb, A.(1960), "A Mathematical Treatment of One-Dimensional Soil Consolidation", Quarterly of Applied Mathematics, Vol. X VI, No. 4, January
9. Monte, J. L. and Krizek, R. J.(1976), "One-Dimensional Mathematical Model for Large-Strain Consolidation", Geotechnique, Vol. X X VI, No. 3, September.
10. Samarasinghe, Mahinda, Huang, Yang H., and Drnevich, Vincent P.(1982), "Permeability and Consolidation of Normally Consolidated Soils" , Journal of Geotechnical Engineering Division, Vol. 106, No. GT6, June.
11. Schiffman, Robert L.(1980), "Finite and Infinitesimal Strain Consolidation", Journal of Geotechnical Engineering Division, Vol. 106, No. GT2, February.
12. Schiffman, R. L. and Cargill, K. W.(1981), "Finite Strain Consolidation of Sedimenting Clay Deposits", Proceedings of Tenth International Conference on Soil Mechanics and Foundation Engineering, Vol. 1, Stockholm.
13. Zhao, Peng(1989), "Analysis of Prefabricated Wick Drains by Uncoupled Finite Strain Consolidation Theory", M. S. Thesis, South Dakota School of Mines and Technology, Rapid City, South Dakota, U.S.A.

(received on Apr, 7, 1997)